Computer-aided detection of wall motion abnormalities in cardiac MRI

Suinesiaputra, A.

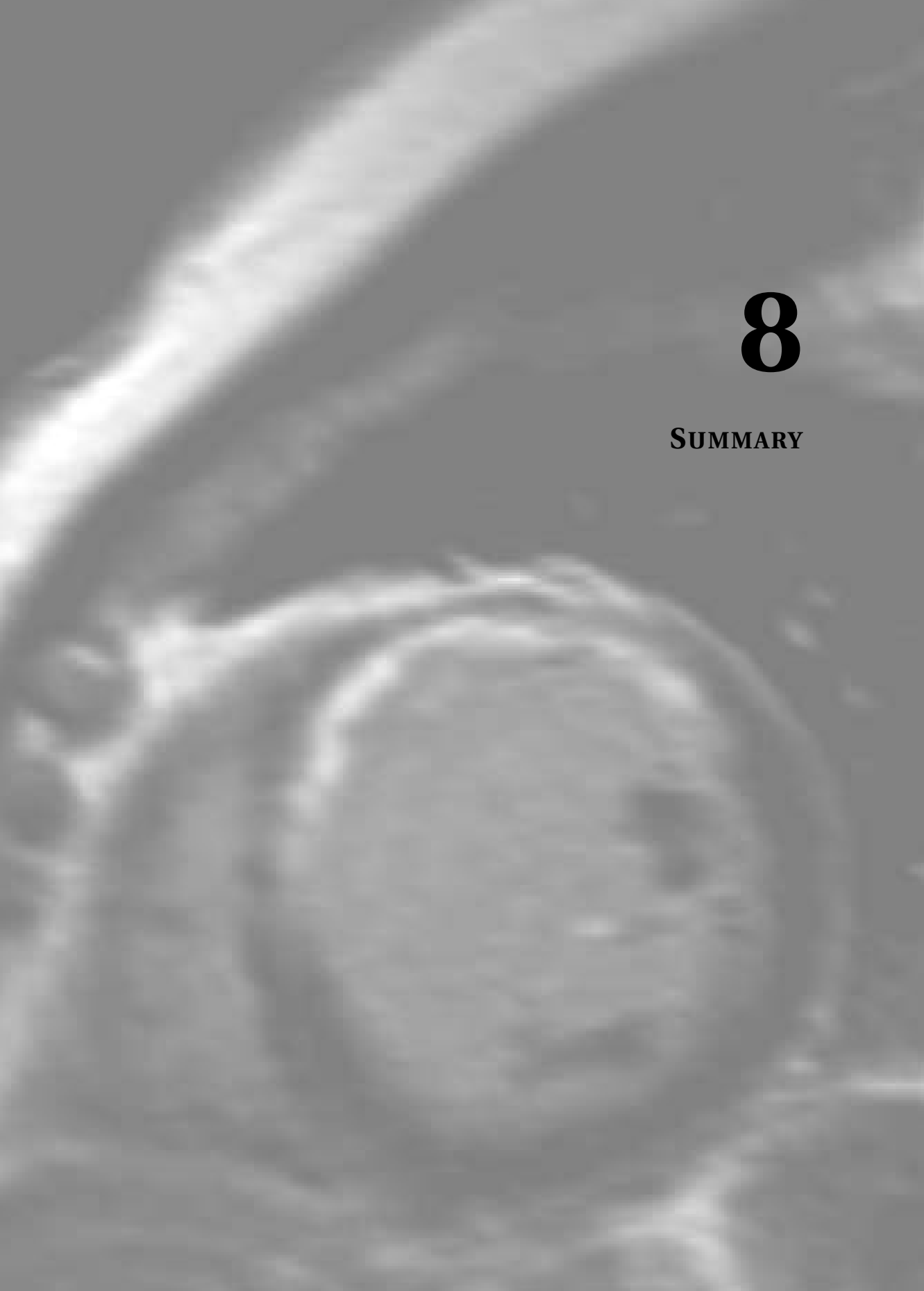

8

SUMMARY

Columbus is not the only person who has
discovered a new continent. So too have I.

Anak Semua Bangsa (Child of All Nations)
PRAMOEDYA ANANTA TOER

8.1 Myocardial wall motion modeling

THE first objective of this thesis was to explore possible shape parameterizations to model normal myocardial contraction. Two different approaches to extract wall motion patterns were presented in this thesis. Chapter 2 presented a study towards direct velocity vector field quantification from tagged MRI, while in Chapter 3, myocardial contractility patterns were extracted from landmark-based endocardial and epicardial contours.

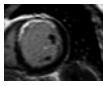

MR tagging allows full inspection of wall motion, not only for myocardial borders, but for all pixels inside the myocardium. The spatially induced tag patterns in MR tagging follow the deformation of the heart, allowing quantification of myocardial deformation fields. Dense velocity vector fields of myocardium can be extracted automatically by using the first order density multiscale optic flow method. This dense optic flow framework does not assume constant pixel intensity, but a constant integral of pixel intensities over a region (local "intensity mass" preservation). It is therefore relatively robust with respect to the problem of decaying intensity of the tag patterns over the cardiac cycle.

In Chapter 2, the proposed dense optic flow method was compared to velocity-encoded (VEC) MRI. Experimental results show strong correlation in the radial direction, but not in the circumferential direction. The correlation is also stronger for velocity vectors in the systolic phase compared to the diastolic phase. Further improvements are still required for this method to overcome this problem, for instance by estimating the optic flow field in the frequency domain instead of in the spatial domain [1, 2].

MR tagging is useful for analyzing local myocardial contraction. In clinical practice however, MR tagging is not included in many routine diagnostic imaging protocols for ischemic heart disease. For this reason, we shifted the research focus to the extraction of myocardial contractility patterns from cine MRI.

Myocardial contours from cine MRI, which include epicardial and endocardial borders, are the main prerequisites for analyzing regional and global LV function. Ejection fraction, wall thickening, wall thinning and stroke volume, to name a few, use both contours from the end-diastolic (ED) and end-systolic (ES) phase. To parameterize these contractility patterns in the remainder of this thesis, endo- and epicardial contours were combined serially to form a *myocardial contraction shape*. Equi-angular landmark points were sampled to establish anatomical point-to-point correspondence of shapes between subjects.

In Chapter 3, we investigated the potential of this myocardial contraction shape definition to distinguish between 42 normal and 47 pathological (ischemic) subjects. Two linear generative models were used to decompose the shapes, i.e., Principal Component

Analysis (PCA) and Independent Component Analysis (ICA). In terms of modes of shape variation, PCA produced global shape variations while ICA generated more local shape variations. In terms of discriminating between normal and pathological subjects, only the first component of the PCA model was sufficient to separate the two groups. For the ICA model, 27 out of 35 (77%) components were required to achieve the same discrimination performance.

From this, we concluded that PCA is suitable for shape decomposition because it can produce a compact model. For classification purposes, the PCA decomposition can only discriminate two groups globally. There is no geometrical interpretation of the classification result that can be deduced from the discriminating principal components. ICA may not be suitable to produce a compact representation of a shape model, because all independent components contribute evenly to the model. However, independent components cannot only discriminate shapes between two groups, but also they can locate the position of the shape differences. This locality property makes ICA more suitable than PCA for the detection and localization of regional wall motion abnormalities. Based on this observation, ICA was used in the remaining chapters as the statistical tool of choice to extract local shape features from myocardial shapes.

8.2 Automated evaluation of regional wall motion abnormalities

The second objective of this thesis was to define a good classifier to detect, to locate and to quantify regional wall motion abnormalities (RWMA). Since an independent component intrinsically contains local geometry of where the component lies in the shape domain, each localized shape component is centered around a "central" landmark point and detection of abnormal regions can be performed by selecting the "abnormal components". This study was given in Chapter 4. First, a patient shape was projected onto the ICA model to reveal its independent component coefficients. Probability density functions of the healthy subject coefficient values were estimated by assuming normal distributions. An abnormal component was defined as a component with a coefficient value which lies outside the normal distribution (beyond ± 3 times standard deviation) of coefficient values of a healthy population.

In Chapter 4, a qualitative validation of the automated RWMA evaluation with abnormal independent components was performed on six infarct patients. These abnormal components were mapped onto myocardial regions by using a mixture of Gaussian functions to color-code RWMA values on cine MRI. A comparison was made with the corresponding CE-MRI. All of the six patients showed good visual correlation between the position of segments with high RWMA values and the hyperenhanced (scarred) segments.

The study in Chapter 4 demonstrated that ICA-based RWMA classifiers are capable of detecting and locating RWMA. In Chapter 6, quantification of RWMA was formulated based on probability values and the process of mapping the abnormal components to the shape domain was refined. The probability density functions of healthy coefficient values were propagated into probability density functions of landmark points. Such propagation is allowed because of the statistical independence property of ICA. This propagation re-

sults in a probability density function for each landmark point that is estimated based on all components, integrating contextual information from neighboring landmarks.

Quantitative validations in Chapter 6 were performed with cross referencing experiments. A comparison with visual wall motion scoring (VWMS) was made by using wall thickening as the reference; in that case the automated RWMA method performed significantly better. If VWMS was used as the reference standard, then the automated RWMA method performance was slightly better than wall thickening. This study demonstrated the capability of the ICA model for detecting segments with abnormal regional wall motion.

8.3 Automated prediction of functional improvement

The last objective of this thesis was to correlate the automated RWMA evaluation method with indicators that may predict functional improvement. Hence, contours from dobutamine stress MR (DSMR) images were used and their RWMA values were compared with RWMA from resting (baseline) MRI. Research hypothesis was that when two myocardial contraction shapes from rest and stress MR from the same patient are evaluated with the ICA-based RWMA method, then the differences in RWMA values could be indicative for myocardial viability.

The pilot study described in Chapter 5 compared the probability values derived from rest and stress contours of independent components that were classified as abnormal. A qualitative comparison in six patients suffering from myocardial ischemia revealed that when contraction from rest to stress improved, the automatically estimated RWMA probability values of abnormal components decreased from rest to stress. An interesting observation was that the automated method detected an improved wall thickening from rest to stress as abnormal for a dyskinetic segment. This fact shows that the automated RWMA method not only incorporates information on wall thickening, but also on wall motion.

In Chapter 7, the methodology was further improved to allow proper comparison of myocardial contraction shapes at stress with baseline (rest) shapes. After rigid (Procrustes) and non-rigid (thin-plate splines) registrations, another non-rigid registration (also with thin-plate splines) was applied to eliminate shape variations at epicardial contours. Hence, only relative motion from endocardial contours with respect to epicardium was modeled. Without this additional registration, false positive samples could occur because strong myocardial contractions at stress could be classified as abnormal.

To quantitatively validate the method for predicting myocardial viability, longitudinal pre- and post-revascularization data is required. However, such data was not available. In Chapter 7, the combination of rest and stress RWMA values was therefore correlated against infarct transmurality from CE-MRI, because CE-MRI is also used to predict functional recovery after revascularization [3]. The automated RWMA probability values achieved strong positive correlation with infarct transmurality in all slice levels. RWMA probability values from the combined rest-stress data progressively decrease as infarct transmurality increases. The method shows high accuracy in the detection of myocardial segments with scar tissue, as confirmed in a validation against CE-MRI.

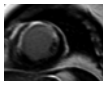

8.4 Future directions

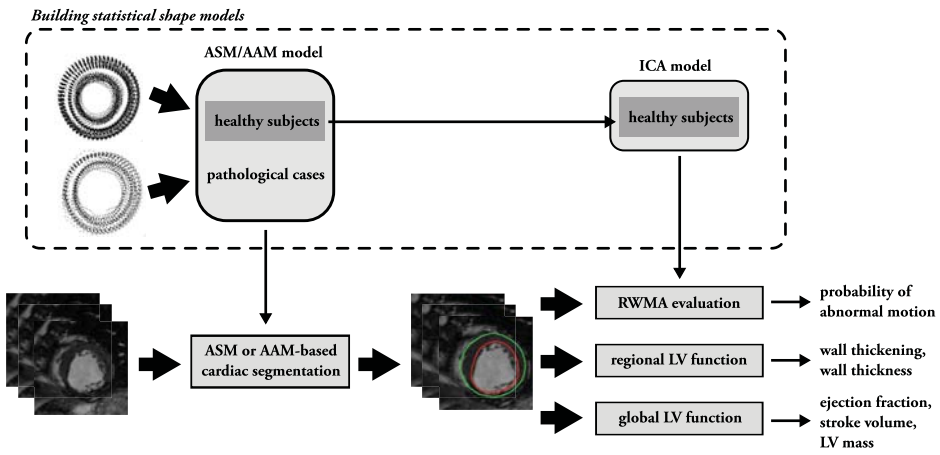

FIGURE 8.1: Pipeline of an automated analysis of cardiac MR images from segmentation to the interpretation of diagnostic values, i.e., RWMA, global and regional LV function, by using statistical shape models.

This thesis presented a number of steps towards the development of automated wall motion analysis to assist in the diagnosis of ischemic heart disease. Further improvements and extensions can be made in several ways. These include the extension of the shape model into a three-dimensional surface of the left ventricle, the inclusion of more temporal samples, and a validation against pre and post revascularization data to properly assess the method's performance for classifying viable tissues.

The presented automated method would fit perfectly at the end of a cardiac MR image processing pipeline for cardiac MRI decision support. Currently, the studies reported in this thesis used manually drawn contours as input. In the future, these myocardial contours could be detected from an automated segmentation method, regardless of the underlying segmentation algorithm. It would be more appropriate to connect components in the pipeline with statistical shape models. For instance, morphometrics based segmentation methods, such as Active Shape Models [4–6] and Active Appearance Models [7, 8], could be used in this pipeline. The ASM/AAM parameters of the segmentation can be used for building a normokinetic model. Figure 8.1 displays how a fully automatic pipeline of cardiac MR analysis with statistical shape models could be realized in this way.

The CAD methods described in this thesis are based on contours from cardiac MRI, but the underlying algorithm does not depend on the imaging modality. The presented method could therefore be used for the diagnosis of RWMA in e.g. echocardiography, but this will require further experimental studies.

Diagnostic results from the automated RWMA evaluation method could also be combined with other diagnostic imaging modalities, for example in a combination of cine MRI

and MR perfusion imaging, FDG-PET imaging, gated SPECT imaging and/or contrast-based images (CE-MRI or MCE). Also information on myocardial deformation could be derived from MR tagging, strain-encoded MR, velocity-encoded MRI or color Doppler echocardiograms. The integration of information on contraction, deformation and perfusion may be a next step towards a more comprehensive CAD method for ischemic heart disease.

8.5 References

[1] L. Florack, H. van Assen, and A. Suinesiaputra, "Dense multiscale motion extraction from cardiac cine MR tagging using HARP technology," in *IEEE 11th International Conference on Computer Vision, ICCV*, 2007, pp. 1–8.

[2] H. C. van Assen, L. M. Florack, A. Suinesiaputra, J. J. Westenberg, and B. M. ter Haar Romeny, "Purely evidence based multiscale cardiac tracking using optic flow," in *Proc. Computational Biomechanics for Medicine II. A MICCAI 2007 Workshop*, 2007.

[3] T. A. M. Kaandorp, J. J. Bax, J. D. Schuijf, E. P. Viergever, E. E. van Der Wall, A. de Roos, and H. J. Lamb, "Head-to-head comparison between contrast-enhanced magnetic resonance imaging and dobutamine magnetic resonance imaging in men with ischemic cardiomyopathy," *Am J Cardiol*, vol. 93, no. 12, pp. 1461–4, Jun 2004.

[4] H. van Assen, M. Danilouchkine, A. Frangi, S. Ordas, J. Westenberg, J. Reiber, and B. Lelieveldt, "SPASM: A 3D-ASM for segmentation of sparse and arbitrarily oriented cardiac MRI data," *Medical Image Analysis*, vol. 10, no. 2, pp. 286–303, APR 2006.

[5] H. C. van Assen, M. G. Danilouchkine, M. S. Dirksen, J. H. C. Reiber, and B. P. F. Lelieveldt, "A 3-D active shape model driven by fuzzy inference: application to cardiac CT and MR," *IEEE Trans Inf Technol Biomed*, vol. 12, no. 5, pp. 595–605, Sep 2008.

[6] M. Uzumcu, R. J. van der Geest, M. Sonka, H. J. Lamb, J. H. C. Reiber, and B. P. F. Lelieveldt, "Multiview active appearance models for simultaneous segmentation of cardiac 2- and 4-chamber long-axis magnetic resonance images," *Invest Radiol*, vol. 40, no. 4, pp. 195–203, Apr 2005.

[7] S. C. Mitchell, J. G. Bosch, B. P. F. Lelieveldt, R. J. van der Geest, J. H. C. Reiber, and M. Sonka, "3-D active appearance models: segmentation of cardiac MR and ultrasound images," *IEEE Trans Med Imaging*, vol. 21, no. 9, pp. 1167–1178, Sep 2002.

[8] E. Oost, G. Koning, M. Sonka, P. V. Oemrawsingh, J. H. C. Reiber, and B. P. F. Lelieveldt, "Automated contour detection in X-ray left ventricular angiograms using multiview active appearance models and dynamic programming," *IEEE Trans Med Imaging*, vol. 25, no. 9, pp. 1158–1171, Sep 2006.